

¹ Bayesian inference of prehistoric population dynamics from multiple
² proxies: a case study from the North of the Swiss Alps

³ Martin Hinz^{1,2,*} Joe Roe¹ Julian Laabs³ Caroline Heitz³ Jan Kolář^{4,5}

⁴ 30 Mai, 2022

⁵ **Abstract**

Robust estimates of population are essential to the study of human–environment relations and socio-ecological dynamics in the past. Population size and density can directly inform reconstructions of prehistoric group size, social organisation, economic constraints, exchange, and political and social institutions. In this pilot study, we present an approach that we believe can be usefully transferred to other regions, as well as refined and extended to greatly advance our understanding of prehistoric demography. Here, we present a Bayesian hierarchical model that uses Poisson regression and state-space representation to produce absolute estimates of past population size and density. Using the area North of the main ridge of the Swiss Alps in prehistoric times (6000–1000 BCE) as a case study, we show that combining multiple proxies (site counts, radiocarbon dates, dendrochronological dates, and landscape openness) produces a more robust reconstruction of population dynamics than any single proxy alone. The model's estimates of the credibility of its prediction, and the relative weight it affords to individual proxies through time, give further insights into the relative reliability of the evidence currently available for paleodemographic research. Our prediction of population development of the case study area accords well with the current understanding in the wider literature, but provides a more precise and higher-resolution estimate that is less sensitive to spurious fluctuations in the proxy data than existing approaches, especially the popular summed probability distribution of radiocarbon dates. The archaeological record provides several potential proxies of human population dynamics, but individually they are inaccurate, biased, and sparse in their spatial and temporal coverage. Similarly, current methods for estimating past population dynamics are often simplistic: they work on limited spatial scales, tend to rely on a single proxy, and are rarely able to infer population size or density in absolute terms. In contemporary demography, it is becoming increasingly common to use Bayesian statistics to estimate population trends and project them into the future. The Bayesian approach is popular because it offers the possibility of combining heterogeneous data, and at the same time quantifying the uncertainty and credibility attached to forecasts. These same characteristics make it well-suited to applications to archaeological data in paleodemographic studies.

³⁰ ¹ Institute of Archaeological Sciences, University of Bern

³¹ ² Oeschger Centre for Climate Change Research, University of Bern

³² ³ CRC 1266 - Scales of Transformation, University of Kiel

³³ ⁴ Department of Vegetation Ecology, Institute of Botany of the Czech Academy of Sciences

³⁴ ⁵ Institute of Archaeology and Museology, Faculty of Arts, Masaryk University

³⁵ * Correspondence: Martin Hinz <martin.hinz@iaw.unibe.ch>

³⁶ Keywords: Prehistoric demography; Bayesian modelling; Multi-proxy; Settlement dynamics

³⁷ Highlights: - Bayesian modelling can integrate multiple, heterogeneous population proxies from the archaeological record - Our initial model produces more robust, high-resolution estimates of past population dynamics than previous, single-proxy approaches - We provide absolute estimates of population size and density on the area north of the Swiss Alps in prehistoric times (6000–1000 BCE)

41 1. Introduction

42 Prehistorians have long recognised demography as a fundamental force in human cultural evolution (Childe,
43 1936). Despite decades of interest in the population dynamics of prehistoric societies, concrete estimates
44 of population size and density before written records remain elusive. Though the archaeological record
45 provides multiple possible demographic proxies (Müller and Diachenko, 2019), a lack of access to this data
46 and methodological tools for turning it into quantitative estimates has left the conclusions drawn from it
47 vague and superficial (Hassan, 1981). As a result, ‘expert estimates’ transferred from ethnographic parallels
48 have often taken the place of direct inference from archaeological evidence Turchin et al. (2015).

49 Prehistoric demography has experienced a resurgence in interest in recent years (Riede, 2009 and others in
50 same issue; Shennan, 2000), partly explained by a renewed interest in human–environment relations and
51 human impact, necessarily requiring an assessment of population size. Kintigh et al. (2014) list human
52 influence, dominance, population size, and population growth amongst their ‘grand challenges’ for archaeology
53 in the 21st century.

54 In particular, the ‘dates as data’ technique (Rick, 1987), using the frequency of radiocarbon dates as a proxy
55 for population dynamics, has been significantly developed in the last decade (e.g. Shennan et al., 2013) and
56 widely applied to archaeological contexts worldwide (Crema, 2022). This approach has contributed greatly to
57 our understanding of prehistoric demography, but is not without its critics Carleton and Groucutt (2021).
58 While the methodology continues to evolve and address these critiques (Crema, 2022), it remains subject
59 to fundamental problems common to all approaches relying on a single proxy Schmidt et al. (2021). We
60 believe that these problems cannot be overcome by methodological refinements in this area alone. Instead, a
61 Bayesian approach offers a robust, quantitative methodology for inferring prehistoric population dynamics
62 from multiple proxies, including summed radiocarbon dates.

63 2. Background

64 2.1. Population estimation in prehistory

65 Proxies currently used for the estimation of population size in prehistory (following Müller and Diachenko, 2019)
66 can roughly be divided into three groups: ethnographic analogies; deductive estimates from ecological/economic
67 factors; and the interpolation of frequencies of archaeological features (e.g. settlements, structures, individual
68 finds). Three basic problems are common to all these approaches:

- 69 1. **Reliance on single proxy:** Most investigations use only one source of evidence. Although multi-proxy
70 approaches exist, the individual proxies only serve to support each other or the main estimator, without
71 explicitly combining them.
- 72 2. **Uncertainty in measurements:** All archaeological evidence is inherently uncertain which is carried
73 through to derived measurements. However, in most studies, single curves are presented as estimates,
74 and the potential error associated is almost never specified.
- 75 3. **Lack of a transfer function:** By ‘transfer function’, we mean something that allows for the proxy data
76 to be interpreted in terms of actual population size or density. This could be absolute, i.e. a numerical
77 estimate of population, or relative, i.e. a means of scaling changes in the proxy value to changes in
78 population. Lack of suitable frameworks and ‘calibration’ data means that this is rarely presented
79 alongside proxy estimates. In the best cases, there is a qualitative assessment of the informative value
80 of the proxy, not sufficiently accounting for the complex nature of archaeological data.

81 Furthermore, the types of archaeological data commonly used as population proxies share a number of
82 problematic characteristics, being:

- 83 • **Limited:** We have only incomplete data, and it is usually not very informative.
- 84 • **Unevenly distributed:** For example, although there is a good data on settlement frequencies for
85 some regions, these regions are very unevenly distributed over time and space.
- 86 • **Noisy:** Frequently individual proxies are strongly influenced by factors unrelated to population, for
87 example taphonomic conditions or depositional biases.

- 88 • **Unreliable:** Research strategies, research history and varying levels of resources available to researchers
 89 strongly affect the nature of compiled datasets. Systematic distortions are the rule rather than the
 90 exception.
- 91 • **Heterogeneous:** All potential proxies have different spatio-temporal scales, granularity, information
 92 value, scales, and data formats.
- 93 • **Indirect:** We will never have direct data on prehistoric population; only proxy data that is thought to
 94 be a reasonable substitute. The transfer functions linking the proxy data with the desired quantity
 95 (population) are unknown.
- 96 • **Contradictory:** When considering several proxies, differences in transfer functions, data quality and
 97 noisiness inevitably lead to different results.
- 98 Many, if not all, of these problems can be ameliorated through a) the explicit, quantitative integration of
 99 multiple proxies; and b) the use of a Bayesian approach to take account of and estimate uncertainty.

100 2.2. Hierarchical Bayesian demographic models

101 Many of the problems with archaeological population proxies are shared with contemporary demography. In
 102 response, demographers have increasingly turned to Bayesian methods to estimate and forecast contemporary
 103 population dynamics. For example, Bryant and Zhang (2018) consider Bayesian data modelling a solution
 104 to exactly the kind of problems that affect archaeological data. Bayesian approaches are well suited for
 105 limited, unreliable and noisy data. Various data sources, even contradictory data, can be brought into a
 106 common framework and used to support one another. These methods also provide a quantitative estimate of
 107 the likelihood and uncertainty of the model's resulting predictions (or in our case retro-dictions). Bayesian
 108 approaches are also capable of accounting for spatially and temporally incomplete data: where this data
 109 is missing, the uncertainty increases, but this does not prevent general modelling and estimation. Finally,
 110 hierarchically-structured model suites, with sub-models for each individual proxy, can be used to estimate
 111 transfer functions between them and the value to be modelled, thanks to the interaction of a large number of
 112 evidence.

113 This modeling technique can thus be used to join different lines of evidence horizontally and vertically and
 114 combine their results into a overall estimate, including an assessment of their reliability: contradicting data
 115 lead to a lower overall reliability, while a mutual support to smaller confidence intervals. If there is no
 116 systematic bias that affects all data sources to the same extent, this results in the most reliable estimate
 117 possible through the most heterogeneous set of data sources.

118 Bayesian radiocarbon calibration is a similar, well-established application in archaeology, where radiometric
 119 uncertainty is modelled based on prior stratigraphic information. More recently, archaeologists have also
 120 used Bayesian modelling techniques for testing hypotheses relating to demographic models based on ^{14}C data
 121 (e.g. Crema and Shoda, 2021). This approach differs from the one presented here in that, in these analyses,
 122 deductive models are generated and their plausibility is tested on the basis of ^{14}C data only. This is a clear
 123 step forward to a model-based, scientific analysis. However, the use of only one proxy, exclusively for testing
 124 hypotheses developed independently, creates problems comparable to those of the inductive approaches used
 125 so far: lacking a combination with other indicators, one is limited to the problems and conditions of sum
 126 calibration. Furthermore, this approach loses significant potential information that would be gained by a
 127 direct evaluation of time series.

128 We attempt to make Bayesian hierarchical techniques usable for archaeological reconstructions. We want to
 129 show, in a reproducible and practical form using a case study, how Bayesian methods can make a decisive
 130 contribution to a better assessment of population development, crucial for the reconstruction of the human
 131 past, even in for periods for which we only have very patchy, noisy and unreliable data.

132 2.3. The Bayesian approach

133 Bayesian statistics relies on the premise that there is always some prior assumption, even if very rough,
 134 about the probability of an event. This assumption is adjusted by observing data, by checking how credible
 135 these priors are (likelihood, see also Bryant and Zhang, 2018, p. 66). This is Bayesian updating (cf. also

136 Kruschke, 2015, especially 15–25), resulting in the posterior probability distribution, which represents not a
137 point prediction. Small amounts of data lead to a broad distribution not strongly localised and restricted.
138 Thus, we simultaneously obtained a result and an estimate the credibility interval, given the data.

139 This Bayesian learning is iterative and sequential, so that the result of one Bayesian inference can form the
140 prior of another (Kruschke, 2015, p. 17). This allows different information to be combined (Bryant and
141 Zhang, 2018, pp. 219–224), as it has long been exploited by archaeology in using stratigraphic information to
142 make radiometric dating more accurate (Ramsey, 1995).

143 This also makes a hierarchical formulation of problem domains possible. Parameters that are necessary for an
144 estimation, such as the relationship of population density to the deforestation signal in pollen data, need
145 not be specified explicitly, but can be given by probability distributions and then estimated in the model
146 itself (Bryant and Zhang, 2018, p. 186). The more data available, the more degrees of freedom can be
147 estimated with a reasonable width of credibility intervals (Kruschke, 2015, p. 112). For the estimation of
148 these parameters, submodels have to be created describing the relationship of the data to the characteristics
149 of the parameter (Kruschke, 2015, pp. 221–222).

150 3. Materials: population proxy data

151 Our case study area north of the Swiss Alps (Figure 1) covers about one third of Switzerland’s territory and
152 comprises the partly flat, but largely hilly area between the Jura Mountains and the Alps. It is favourable
153 for settlement and agriculture; the Swiss Plateau between Lake Zurich and Lake Geneva is by far the most
154 densely populated region of the Switzerland today. This serves as our core region of interest because it
155 is here that archaeological data is most abundant and accessible. The region has a very diverse natural
156 landscape: shaped by glaciers during the ice ages, the many lakes and bogs provide excellent preservation
157 conditions for the numerous Neolithic and Bronze Age lakeside settlements, and a rich source for vegetation
158 reconstructions by means of pollen analyses. Thanks to the very active and efficient archaeological research
159 and heritage management there is an abundance of archaeological information, including known sites as well
160 as dendrochronological and ^{14}C data.

161 Our case study targets the period between 6000–1000 BCE. The lower limit of this time window was chosen
162 to avoid the so-called ‘Hallstatt plateau’ in the Northern Hemisphere radiocarbon calibration curve, which
163 causes difficulties for the ^{14}C proxy. The upper limit coincides with post-glacial changes in pollen spectra,
164 before which the openness indicator is highly unlikely to reflect human influence.

165 A large number of different proxies can be integrated into a model of this type, provided that these observations
166 a) can be understood as dependent on the population density in the past, and b) a model-like description
167 of this dependence can be created. Table 1 provides a non-exhaustive list. For our case study, we used a
168 landscape openness indicator; an aoristic sum of typological dated sites; a sum calibration; and frequency
169 data for dendro-dated lakeshore settlements in the Three Lakes region (western Swiss Plateau).

Table 1: A incomplete list of possible observation that can be linked
to population developments in the past. Proxies used in this study
are highlighted.

| Proxies |
|-------------------------------------|
| Expert estimates |
| Ethnographic Analogies |
| Carrying Capacity |
| Economic modelling |
| Extrapolation of buried individuals |
| Burial anthropology |
| Settlement data, number of houses |
| Settlement data, settlement size |
| Aoristic analysis |

| |
|---|
| Proxies |
| Dendro dates |
| Amount of archaeological objects |
| Radiocarbon sum calibration |
| Estimates based on specific object types |
| Human impact from pollen or colluvial data |
| aDNA based estimates |
| ... |

170 3.1. Dendro-dated lakeshore settlements

171 From the Neolithic onwards, known settlement areas in Switzerland concentrate along its rivers and lakes
 172 (Christian Lüthi, 2009). Thus, our working region offers excellent data for demographic estimation, but
 173 poses very specific problems for such an undertaking. We have high-resolution information on the temporal
 174 sequence of individual lakeside settlements by means of dendro data. In these cases, ^{14}C data are not as
 175 abundant simply because they are inferior to dendro dating.

176 The dataset we use for the number of dendro-dated wetland settlements in the Three Lakes region was
 177 collected by Julian Laabs for his PhD thesis (Laabs, 2019). The time series used here runs from 3900 to 800
 178 BCE, and contains the number of chronologically registered fell phases at individual settlements.

179 3.2. Summed radiocarbon

180 The dataset for the ^{14}C sum calibration primarily consists of data from the XRONOS database (<https://xronos.ch>), supplemented by dates from the unpublished PhD thesis of Julian Laabs (Laabs, 2019) and the
 181 data collection of Martínez-Grau et al. (2021). It contains a total of 1135 single ^{14}C data from 246 sites
 182 (see Figure 2). The dates in the dataset range in ^{14}C years from 10730 to 235 uncal BP. This time window
 183 extends beyond the study horizon in order to minimise boundary effects.

184 We binned the data at site levels to obtain a temporally dispersed count and thus an expected value of
 185 contemporaneous ^{14}C dated sites. For the creation of the sum calibration, the corresponding functions of the
 186 R package rcarbon (Crema and Bevan, 2021) were used with their default settings.

188 3.3. Aoristic sum

189 We include relative dating information obtained from the heritage authorities of the Swiss cantons (Figure 3).
 190 These are primarily derived from scattered surface finds, often with a low dating accuracy (only in the range
 191 of archaeological periods), incorporated into our model as a typologically-dated, aorist time series. However,
 192 it is not dependent radiocarbon dating and thus it avoids the methodological issues of sum calibration. Data
 193 from 4321 sites were included in the aoristic sum.

194 3.4. Landscape openness

195 Natural conditions in the Swiss lakes enable not only highly precise dating of archaeological sites, but also
 196 a very dense network of pollen analysis. We make use of this by generating a supra-regional openness
 197 indicator for the vegetation from the pollen data (Figure 5). This proxy has the specific advantage that it is
 198 not dependent on archaeological preservation conditions, making it particularly valuable for compensating
 199 systematic distortions that result from archaeological taphonomy and period-specific settlement patterns.

200 We assume that the higher the population density in an area, the greater the human influence on the
 201 natural environment Lechterbeck et al. (2014). Evidence of deforestation can therefore provide indications of
 202 population dynamics. The full procedure for deriving this proxy from several different pollen diagrams is
 203 detailed in a previous publication (Heitz et al., 2021). Here, we use five pollen diagrams from sites mainly in
 204 the hinterland of the large Alpine lakes.

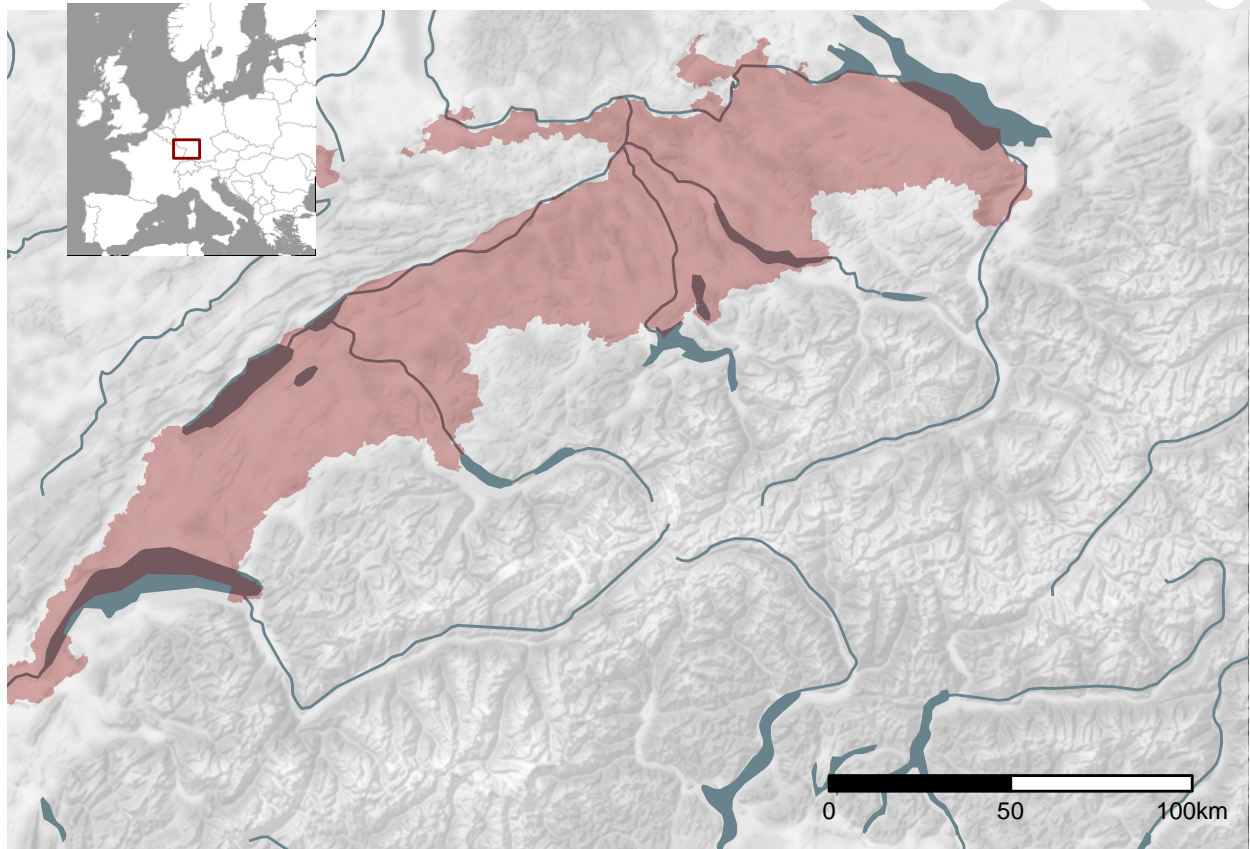


Figure 1: Location and extent of the Swiss Plateau as biogeographical region (based on swisstopo) including additional low altitude areas in the north of Switzerland (regions along the High Rhine between Schaffhausen and Basel).

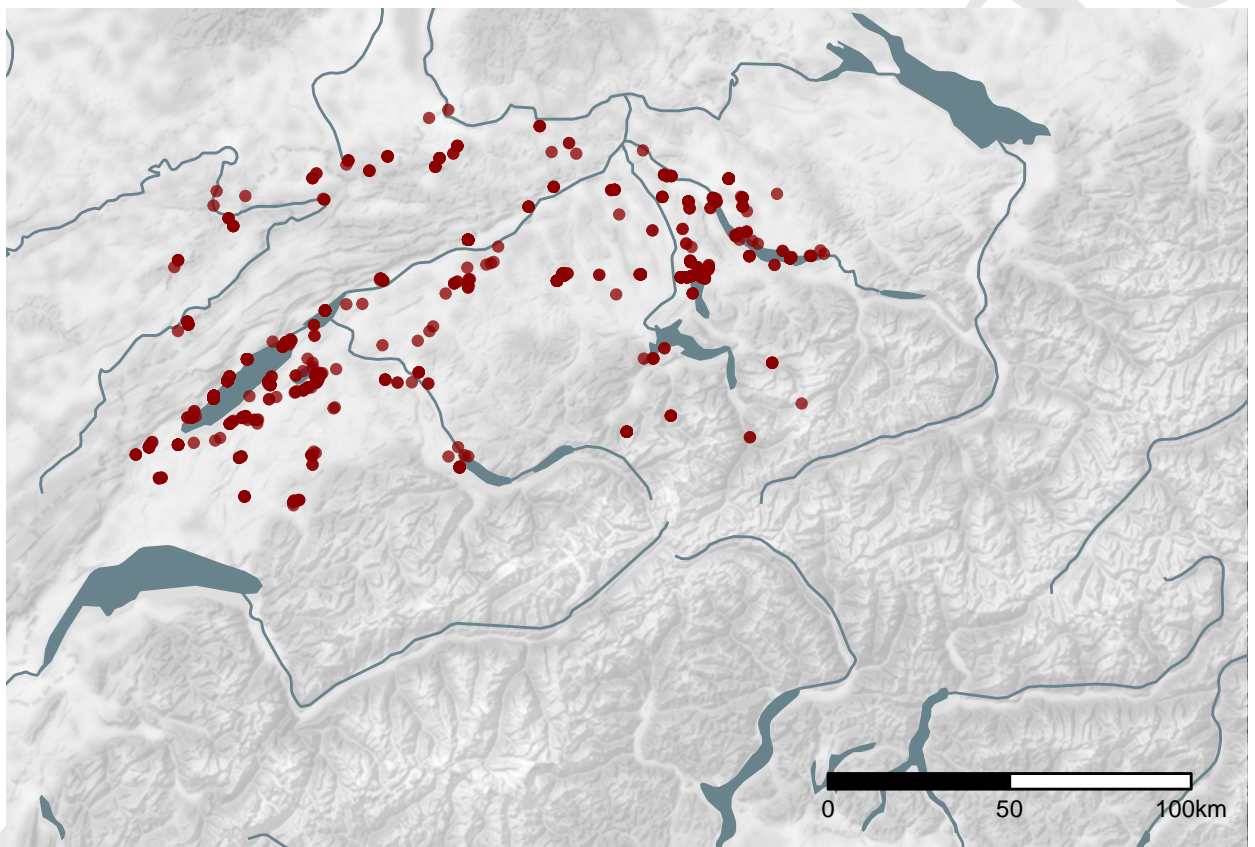


Figure 2: The location of the ^{14}C dated sites in the dataset.

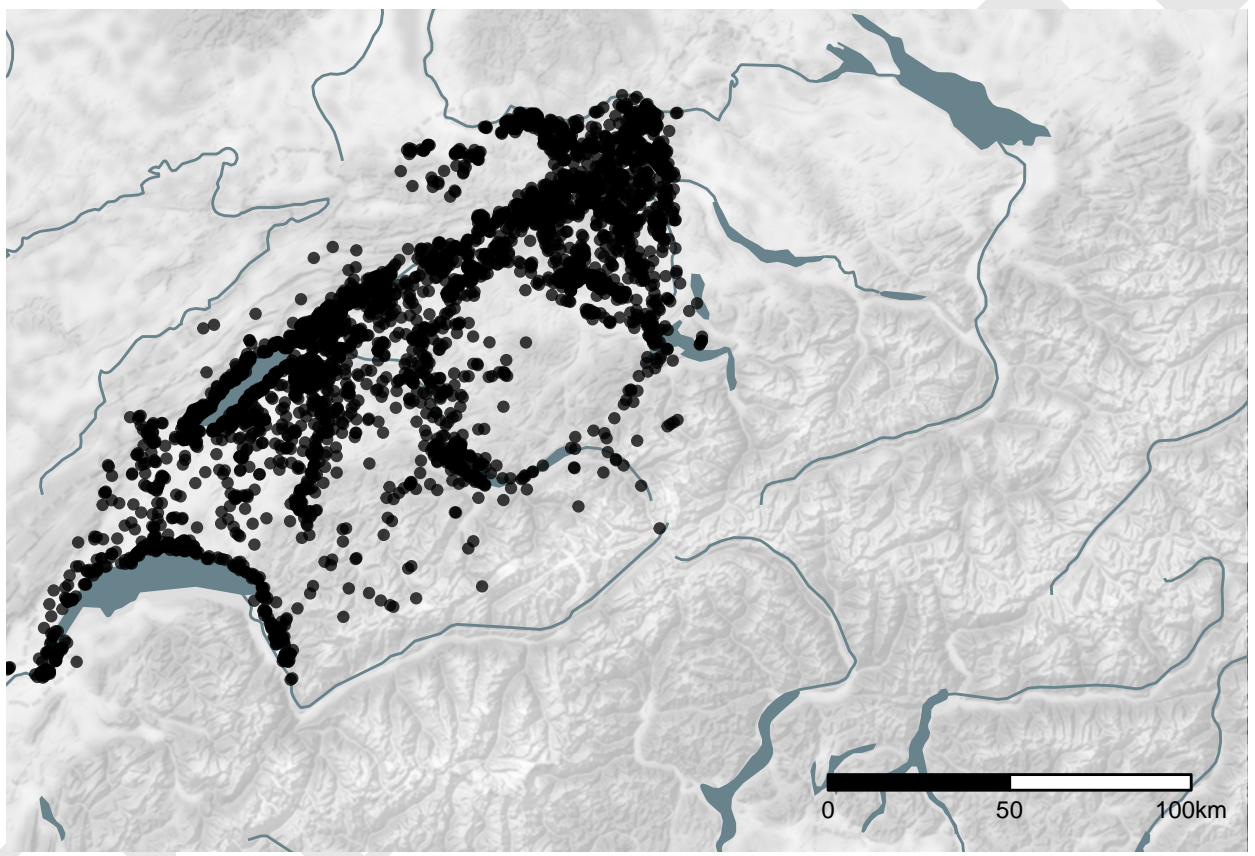


Figure 3: Location of the sites from the find reports of cantonal archaeology (heritage management) authorities. Locations are ‘fuzzed’ by approximately 1 km.

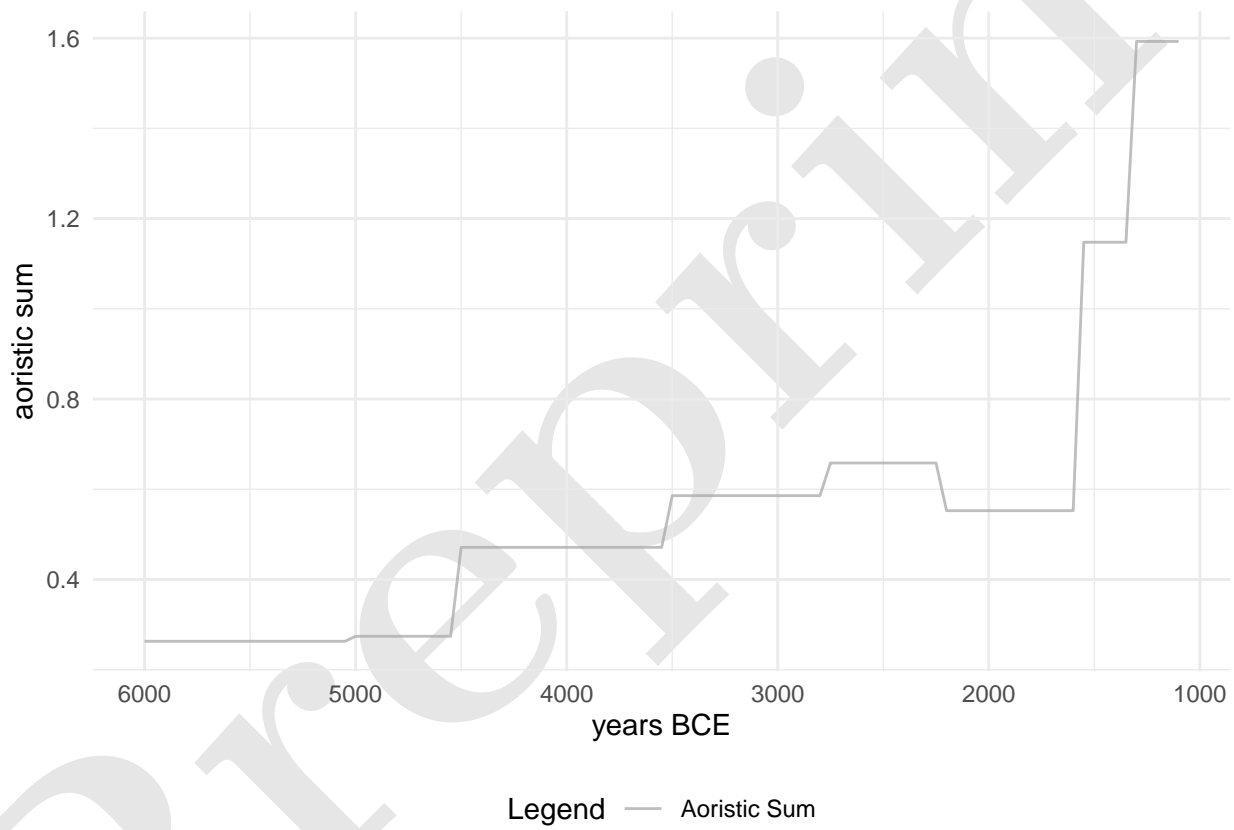


Figure 4: Aoristic sum of archaeological sites used in the analysis.

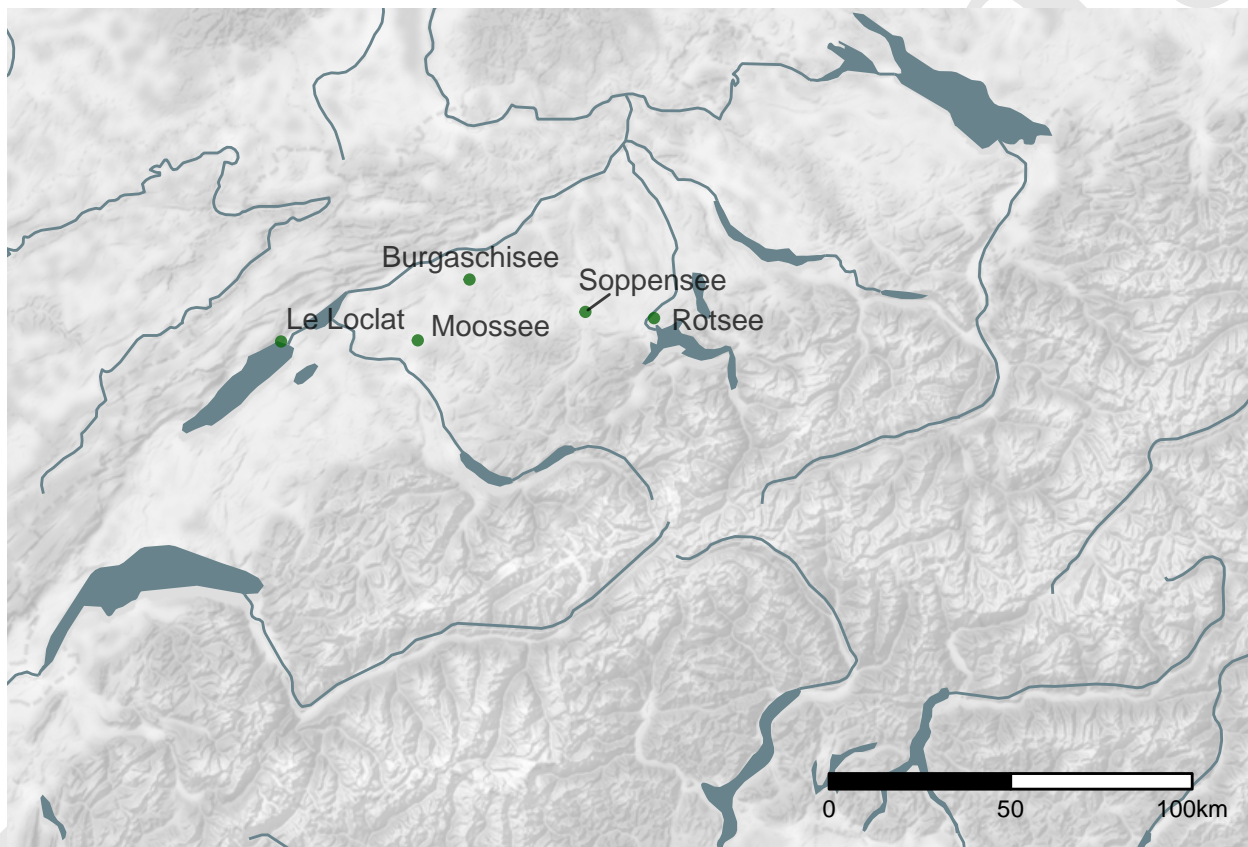


Figure 5: Location of the pollen profiles used for the openness indicator.

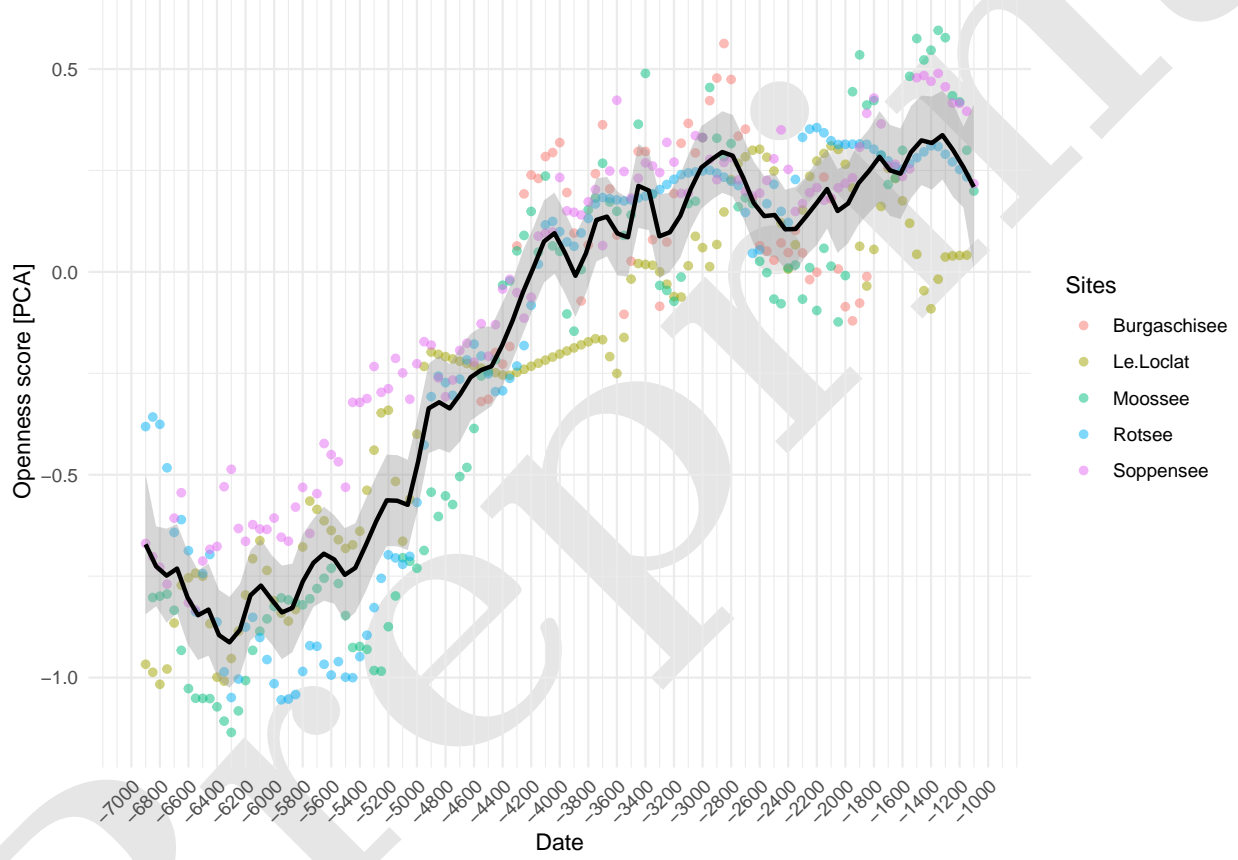


Figure 6: Value on the first dimension of the PCA against dating of the samples for the individual pollen profiles and their combined average value as the openness indicator.

205 **4. Methods: Bayesian model**

206 Sum calibration, openness and the dendro-dated settlement data was smoothed by a moving average with a
207 50 years window, corresponding to the unified sampling interval for all proxies. The aoristic sum was not
208 smoothed, because it already has a very coarse temporal resolution. In the construction of our ‘observational
209 model’, we considered all these proxies as informative of the number of settlements located in the north of
210 the Swiss Alps. Population development is simulated in a ‘process model’ using a Poisson process.

211 **4.1. Process model**

212 A special class of Bayesian hierarchical models are so-called ‘state space models’, specifically designed for
213 time series. They follow two principles. First, a hidden or latent process is assumed, representing the state of
214 the variable of interest x_t through the entire time series. Every state of variable x in the future, as well as in
215 the past, is bound by a Markov process to the state of variable x at time t . Second, it is assumed that certain
216 observations, represented in variable y , are dependent on the state of variable x at time t . This implies that
217 a relationship between the individual states of variable y is generated over time via the hidden variable x ,
218 which is not directly observable.

219 This structure makes these models particularly suitable for demographic reconstruction using archaeological
220 and other data. Population density itself is not directly measurable: all we have at our disposal are observations
221 derived by unknown transfer functions.

222 Our overall model is broken down into several hierarchically-connected individual elements. The a process
223 model represents the demographic development itself, without already being explicitly parameterised with
224 data. Here we assume that the latent variable ‘number of sites’ is strongly autocorrelated across different
225 time periods. The number of sites in 3000 BCE is strongly conditioned by the number of sites in 3050 BCE,
226 and so on. The population at time t results from the population at time $t - 1$ times a parameter λ , which
227 represents the population change at this time.

$$N_t = N_{t-1} * \lambda_t$$

228 A univariate discrete Poisson distribution is particularly suitable for modelling frequencies, numbers of events
229 that occur independently of each other at a constant mean rate in a fixed time interval or spatial area. It is
230 determined by a real parameter $\lambda > 0$, describing the expected value and the variance. Thus, the relationship
231 shown above can be rearranged as follows:

$$\begin{aligned} N_t &\sim dpois(\lambda_t) \\ \lambda_t &= N_t \end{aligned}$$

232 If we now have information about the change in population development (the proxies), this can enter into the
233 model via a change in λ in form of a regression: for all proxy values — represented as a vector of independent
234 variables $x \in R^n$, with R^n as an n-dimensional Euclidean space defined by the n variables — the model takes
235 the form:

$$\log(E(Y | x)) = \alpha + \beta'x$$

236 Using the logarithm as a link function ensures that λ , which must always be positive, can also be described
237 by variables that may also be negative. β serves as slope factor, as in a normal linear regression. Here, it
238 functions as a scaling factor for the individual proxies. α is to be understood as an intercept, representing a
239 baseline when there were no change due to the variables. This is the desired behaviour: λ is equal to the
240 value of the population in the previous time period, plus or minus the changes resulting from the variables.

$$\log(\lambda_t) = \log(N_{t-1}) + \sum_{i=1}^n \beta_i x_{t,i}$$

241 Since λ and N are essentially in the same range (e.g. if $lambda = 1$, the expected value for N would also be 1),
 242 N_{t-1} must also be log-transformed for the congruence of both values. Population size N_t as well as population
 243 change λ_t are time-dependent. At each individual point in time, these variables will take on different values.
 244 But we can assume that the population change will not exceed certain limits (*max_change_rate*), though it
 245 is not possible to specify this at this point.

$$\begin{aligned} max_growth_rate &\sim dgamma(shape = 5, scale = 0.05) \\ N_t/N_{t-1} &< (max_growth_rate + 1) \\ N_{t-1}/N_t &< (max_growth_rate + 1) \end{aligned}$$

246 A gamma distribution centres probability in the range $[0, 1]$; adding 1 makes this range $[1 - 2]$. This prevents
 247 the number of sites from explosively increasing between two time periods, which would lead to problems for
 248 the convergence of the model. The estimation of this parameter for the entire model, as well as the estimation
 249 of the respective population change per time section, results from the modelling and the interaction with the
 250 data.

251 4.2. Observational model

252 In this initial implementation, the observational model is essentially a Poisson regression, where the proxies
 253 are used to inform the change in the number of settlements between time steps. The individual proxies were
 254 z-normalised and absolute differences between time steps were then computed. If the value of the proxy
 255 increases, this results in a positive difference from the previous time step, and vice versa.

$$\begin{aligned} z_t &= \frac{x_t - \bar{x}}{\sigma_x} \mid \sigma_x := Standard\ Deviation \\ \delta z_t &= z_t - z_{t-1} \end{aligned}$$

256 The sum of the resulting differences between the time steps, together with the settlement number of the
 257 previous step as the expected value, then forms λ_t : the expected value for the settlement number of the
 258 current time step.

$$\log(\lambda_t) = \log(N_{t-1}) + \sum_{i=1}^n \beta_i \delta z_{i,t}$$

259 Here, β_i is a scaling factor that represents the influence of the respective proxy. It is a confidence value of the
 260 model for the respective proxy, so that the sum of all β_i results in 1.

$$\sum_{i=1}^n \beta_i = 1$$

261 A Dirichlet distribution—a multivariate generalization of the beta distribution—is commonly used for
 262 this purpose in hierarchical Bayesian modelling. Its density function gives the probabilities of i different
 263 exclusive events. It has a parameter vector $\alpha = (\alpha_1, \dots, \alpha_i) \mid (\alpha_1, \dots, \alpha_i) > 0$, for which we have chosen a
 264 weakly informative log-normal prior. The priors for the log-normal distribution in turn come from a weakly
 265 informative exponential distribution for the mean and a log-nomal distribution with μ of 1 and σ_{log} of 0.1:

$$\begin{aligned}
\beta_i &\sim Dir(\alpha_{1-i}) \\
\alpha_i &\sim LogNormal(\mu_{alpha_i}, \sigma_{alpha_i}) \\
\mu_{alpha_i} &\sim Exp(1) \\
\sigma_{alpha_i} &\sim LogNormal(1, 0.1)
\end{aligned}$$

266 Intuitively, we consider the sum of the proxies as determinant of the number of settlements. That is, the
267 share of each individual proxy is variable and is estimated within the model. This share is recorded within
268 the model as the parameter p.

269 The error value is represented by the Poisson process in the process model. In this implementation, the model
270 finds the best possible combination between the individual proxies to describe a settlement dynamic. The
271 number of sites is converted into population density using (certainly debatable) parameters defined by us,
272 but which are only scaling factors for the intermediate value of number of settlements. We assume that each
273 site represents a number of people that is poisson distributed around the value 50, a compromise, as both
274 Mesolithic and Neolithic and Bronze Age settlement communities need to be represented. An evidence-based
275 estimate data series of the temporal development of settlement sizes could enhance this specification. From
276 the number of sites and the mean number of individuals a population density can be calculated using the
277 case study area (12649 km^2), making the models estimate comparable with estimates from other sources or
278 the literature.

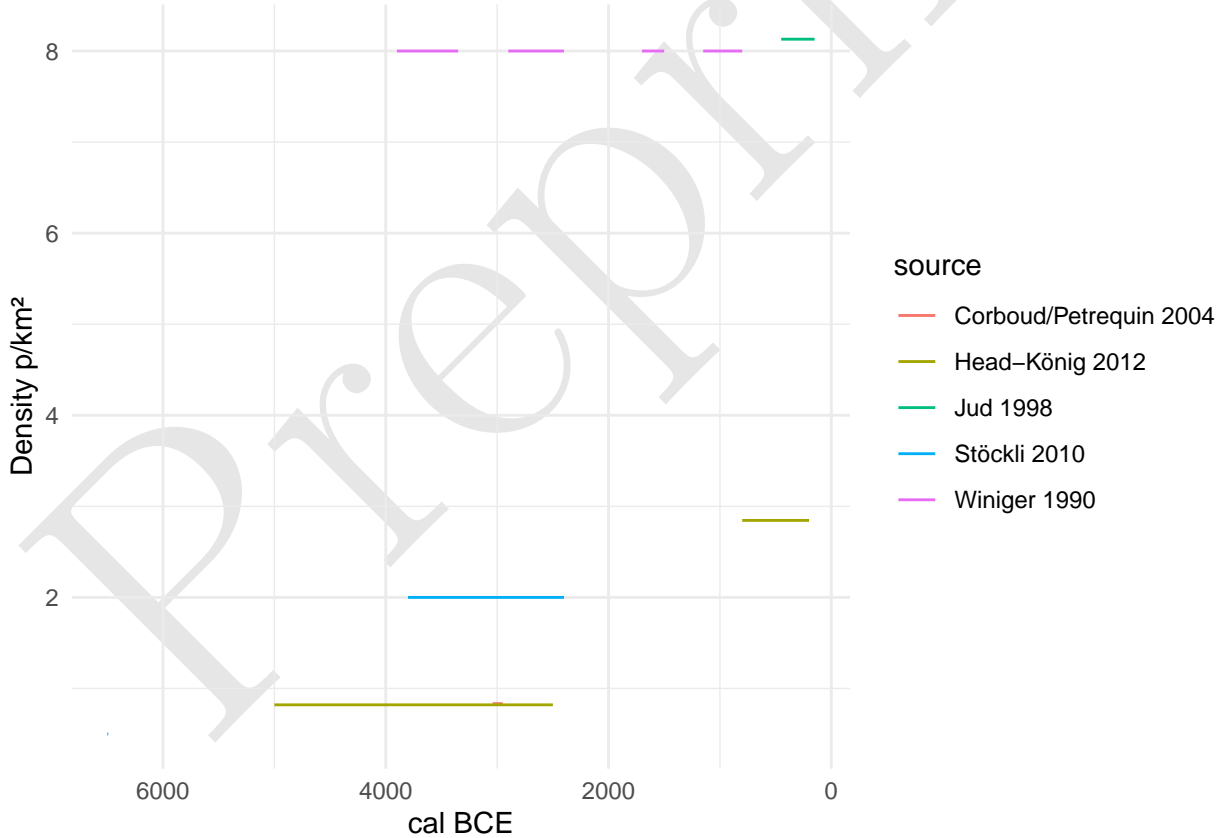


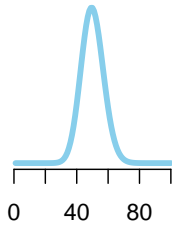
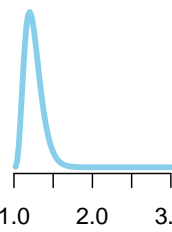
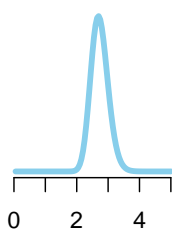
Figure 7: Expert estimate of population density on the Swiss Plateau.

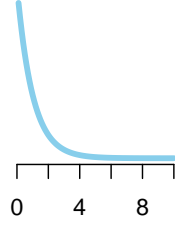
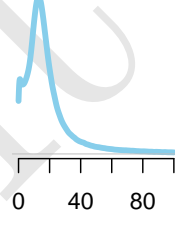
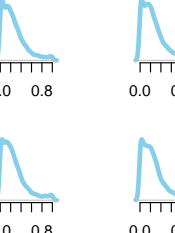
279 4.3. Model fitting

280 The model was fitted using the R package *nimble* (version 0.11.1, R version 4.1.3), using 4 parallel chains.
281 Achieving and ensuring convergence and sufficient effective samples (10000) for a reliable assessment of the

282 highest posterior density interval was carried out in steps.
 283 1) the model was initialised for each chain and run for 100000 iterations (with a thinning of 10). On a
 284 reasonably capable computer (Linux, Intel(R) Xeon(R) CPU E3-1240 v5 @ 3.50GHz, 4 cores, 8 threads),
 285 this takes approximately a minute.
 286 2) the run was extended until convergence could be determined using Gelman and Rubin's convergence
 287 diagnostic, the criterion being that a potential scale reduction factor of less than 1.1 was achieved for
 288 all monitored variables. Convergence occurred after about thirty seconds.
 289 3) Due to the high correlation of the parameters and thus a low sampling efficiency, the collection of at
 290 least 10,000 effective samples for all parameters took about five hours.
 291 A starting value of 5 p/km² for the population density of the Late Bronze Age (1000 BCE) was taken from
 292 the literature, which may represent a general average value for all prehistoric population estimates (Nikulka,
 293 2016, p. 258). For the model, this was set as the mean of a normal distribution with a standard deviation of
 294 0.5, which should give enough leeway for deviations resulting from the data. Nevertheless, it should be noted
 295 that our resulting estimate is strongly conditioned by this predefined value, especially in the later sections.
 296 For traceplots and the prior-posterior overlap, as well as density functions of the posterior samples of the
 297 individual parameters, please refer to the supplementary material.

Table 2: Priors and fixed parameters used in the model.

| Priors | Value | Plot/Comment |
|-----------------|-----------------------------------|---|
| MeanSiteSize | dpois(50) |  |
| max_growth_rate | dgamma(shape = 5, scale=0.05) + 1 |  |
| mu_alpha | dlnorm(1,sdlog=0.1) |  |

| Priors | Value | Plot/Comment |
|-----------------------------|--------------------------------------|--|
| a_alpha | dexp(1) |  |
| alpha | dlnorm(mu_alpha[j],sdlog=a_alpha[j]) |  |
| p | ddirch(alpha[1:4]) |  |
| Parameters | | |
| nEnd | 5 | |
| AreaSwissPlateau | 12649 km ² | |
| Initial Values | | |
| lambda _{1:nYears} | $\log(1 - 10^{\frac{1}{nYears-1}})$ | exponential increase of the factor 10 |
| PopDens _{1:nYears} | nEnd (=5) | |
| nSites _{1:nYears} | 50 | |

298 5. Results

299 The population density estimated by the model (Figure 8) ranges between 0.2 p/km² for the beginning (6000
300 BCE) and 4.8 p/km² for the end of the estimate (1000 BCE), reaching a maximum of 6.5 p/km² for around
301 1250 BCE. This remains within the range considered plausible according to expert estimates. There are
302 clear peaks around 1250 BCE and around 2750 BCE, which corresponds to the beginning of the influence of
303 Corded Ware ceramic styles (Hafner, 2004).

304 The temporal distribution of variability in the estimate (Figure 9) allows us assess at which time steps the
305 uncertainty is greater due to e.g. contradictions in the proxies. The coefficient of variation is 0.13 for the
306 beginning and 0.1 for the end of the estimate, with the greatest variability (0.47) seen around 2150 BCE.
307 This is not surprising as there are fewer archaeological contexts recorded from the earlier phase of the Early
308 Bronze Age, c. 2200-1800 BCE. This picture changes from c. 1800 BCE onwards (David-Elbiali, 2000; Hafner,
309 1995). The beginning and end of the time series are relatively clearly determined, resulting from the *a priori*
310 setting of final population density, but also from the uniformity of the proxies during these periods. Overall,

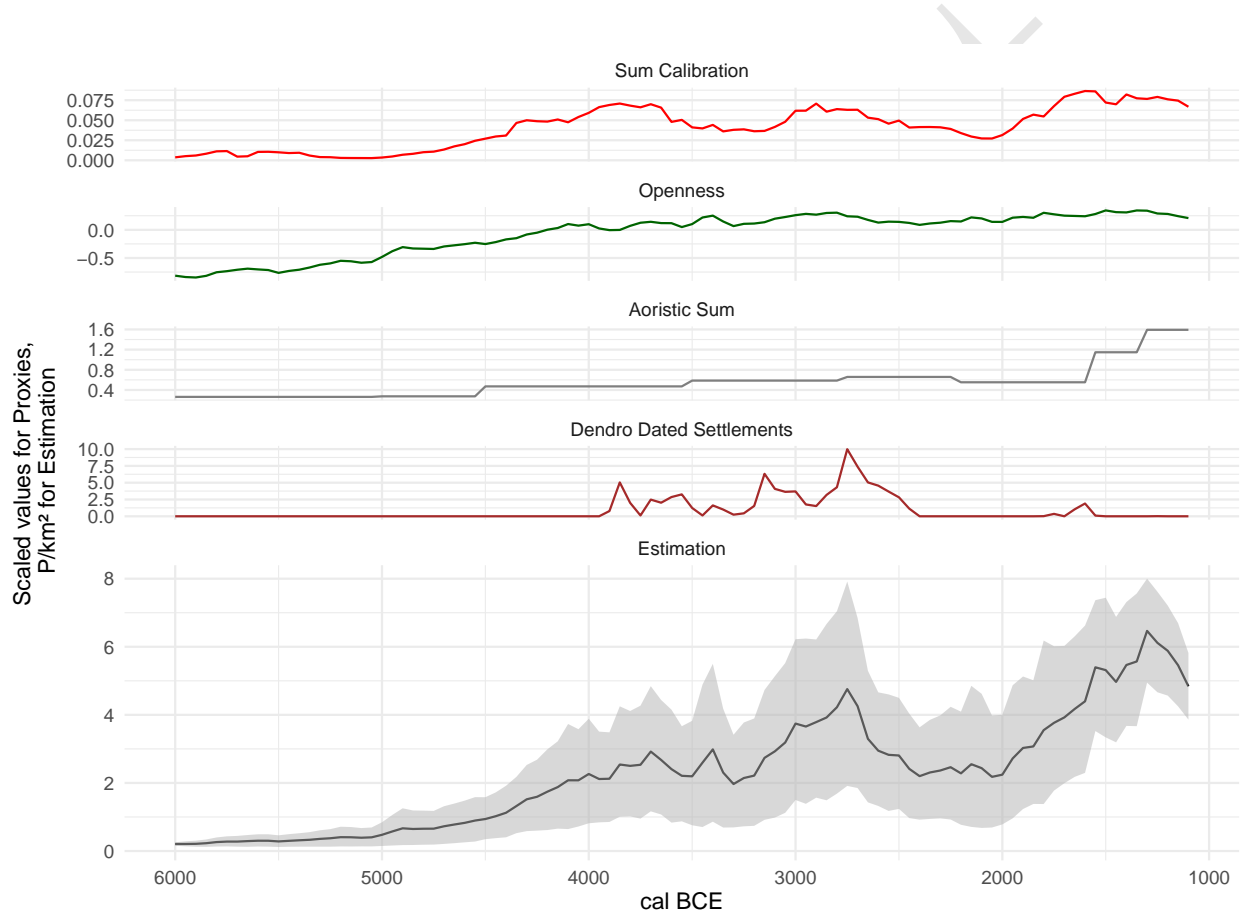


Figure 8: Estimate of population density predicted by the model. The four input proxies are also plotted (scaled) for comparison.

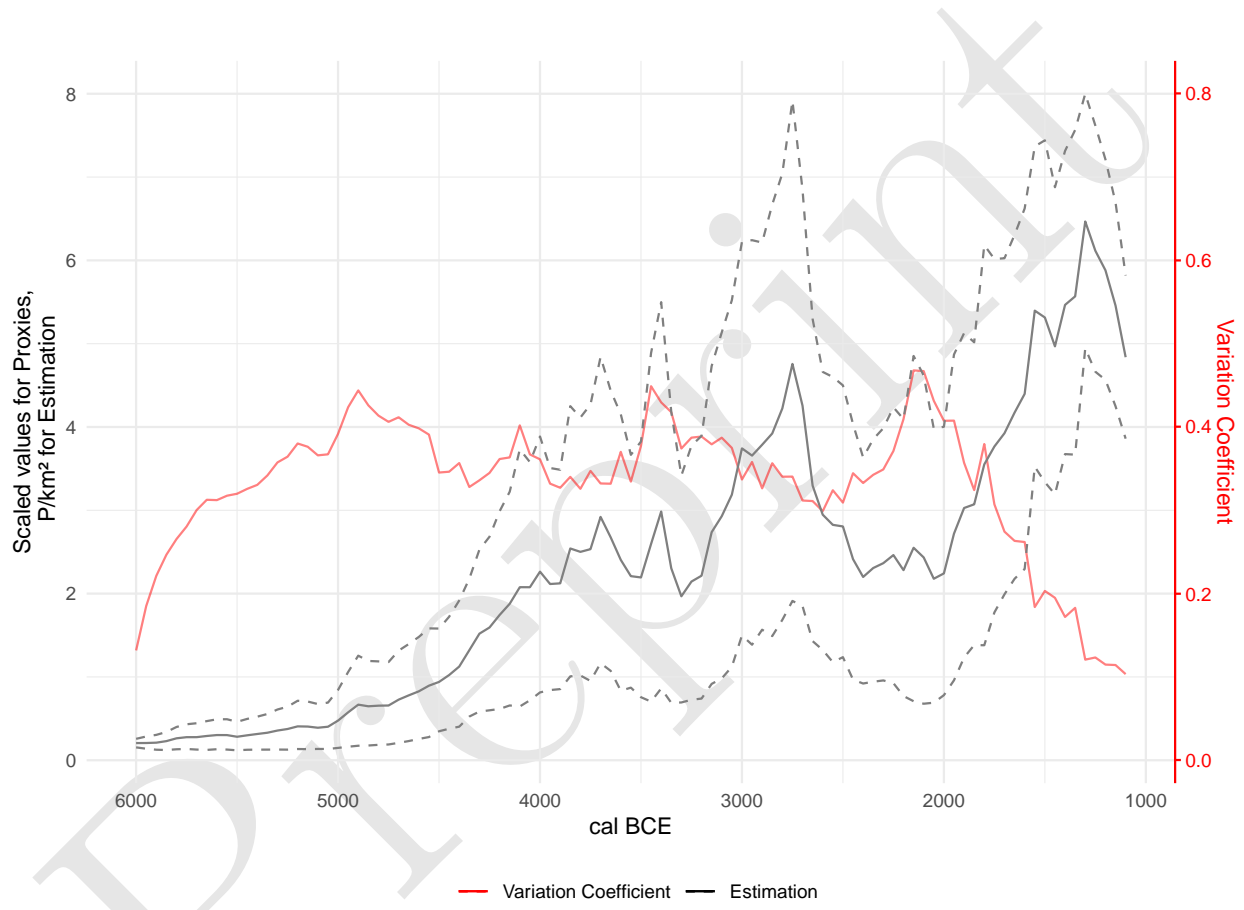


Figure 9: Variability of the model estimate of population density over time, with the estimate itself for reference.

311 the variability is relatively stable over the entire estimation and averages 33% of the respective mean.

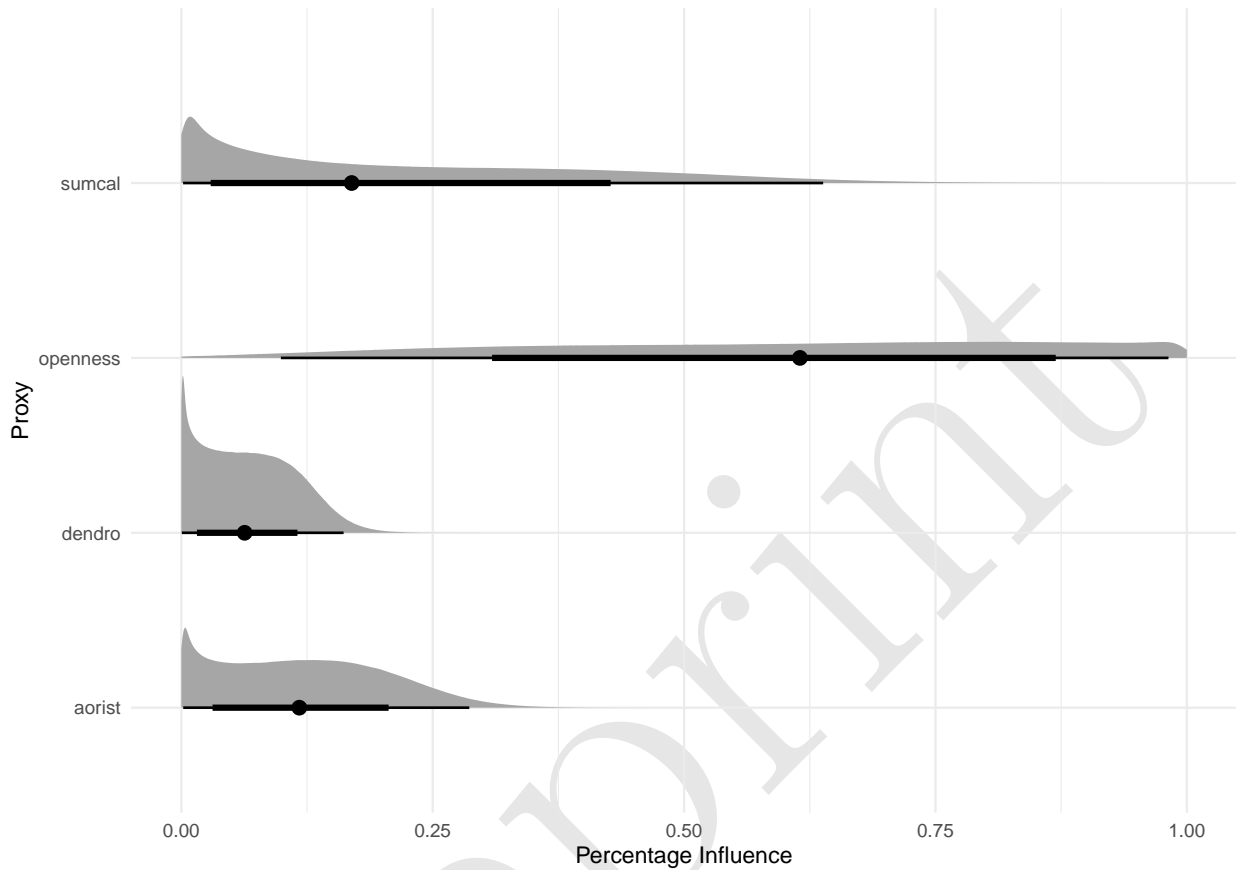


Figure 10: Distribution of influence ratios of proxies on model's final estimation of number of sites.

312 The parameter p reflects the relative weight given to the individual proxies. Its posterior distribution (Figure
313 10) shows that the model weights the openness indicator the highest, averaging slightly above 60%, followed
314 by the sum calibration, with an average of about 20%. The aoristic sum is slightly above 10%, whereas the
315 importance of the dendro-dated settlements is below 10%. The reason for the latter is certainly that there
316 are no lakeshore settlements over large areas of the time window, and therefore the overall confidence in the
317 proxy is low. The aoristic sum is flat for long periods, making it difficult to integrate with other proxies. The
318 sum calibration shows very strong short-term fluctuations, at least partly due to the calibration curve, which
319 suggests that it does not reliably represent a continuous population trend. Its fluctuations have an impact on
320 the model's estimate, albeit to a lesser extent than the general trend.

321 6. Discussion

322 6.1. Reliability of individual proxies

323 Comparing the model's overall estimate with the individual proxies provides several insights into the quality
324 of these records. The sum calibration, currently the most frequently used proxy for (relative) population
325 change in prehistory, has its large fluctuations dampened when considered alongside other proxies. This
326 is especially true of the first fluctuation shortly after 4000 BCE. The expected increase in archaeological
327 remains with the onset of Neolithisation is still clearly visible, but the overall curve is much flatter than
328 the sum calibration itself. The period between 3950 and 3700 BCE, contemporaneous with the first major
329 settlement of the Three Lakes regions' lakeshores, coincides with a noticeable plateau in the calibration curve,

330 producing an overestimation of the ^{14}C density. A second maximum, after 3000 BCE, is supported by the
331 other proxies, and is consequently much more reflected in the overall estimate, coinciding with a smaller and
332 shorter plateau. The rise towards the Middle and Late Bronze Age is also supported by the other proxies,
333 without a significant pattern in the calibration curve. We may conclude that the model is successful in using
334 information from other proxies to sift ‘real’ fluctuations in the summed radiocarbon record from artefacts of
335 the calibration curve.

336 On average, the model weights the sum calibration at about 20%, significantly less than the 60% afforded
337 to the openness indicator. After an initial increase, which is easily explained by spread of agriculture, the
338 openness indicator tends to fluctuate less and thus has a dampening effect on the overall estimate. In general,
339 this trend in the sum calibration is well reflected in land openness, while changes within the Neolithic and
340 Bronze Age are more gradual.

341 The aoristic sum remains flat over long spans of time. It is not until the Middle and Late Bronze Age that
342 we see a significant rise, which is also apparent in the model’s overall estimate. It remains to be seen to what
343 extent modelling of the taphonomic loss (Surovell et al., 2009) could be integrated in this approach.

344 The number of simultaneously existing lakeshore settlements is a temporally and spatially limited estimator,
345 but extremely reliable. Its limitations are reflected in the low overall confidence of the model, since its value
346 is zero over long stretches. However, where it has information potential, such as around and shortly after
347 3800 BCE, 3200 BCE, 1600 BCE or especially around 2750 BCE, its fluctuations have a noticeable influence
348 on the overall estimate. This highlights another potential of our approach: where a proxy has little structure
349 and thus little significance, or where its trends cannot be linked to other indicators, it consequently has little
350 influence. For periods in which it can provide information, however, this will also feed into the overall model,
351 despite a low overall confidence in the estimator.

352 **6.2. Prehistoric population dynamics north of the Swiss Alps**

353 In order to review the reconstruction against the background of established archaeological knowledge, it is
354 useful to overlay conventionally-defined archaeological phase boundaries (Hafner, 2005) on the results of our
355 model (Figure 11).

356 The Early and Middle Neolithic are hardly documented in Switzerland. We must assume a low level of
357 settlement, probably mainly by mobile groups. Isolated Neolithic sites of the LBK and later groups are known
358 in the periphery of Switzerland, but they play a subordinate role (Ebersbach et al., 2012). The evidence
359 of the Neolithic is dense from the so-called Upper Neolithic onwards, connected with the typochronological
360 pottery phases of Egolzwil (late 5th millennium BCE) and Cortaillod respectively Pfyn (first half of the
361 4th millennium BCE). The first lake shore settlements north of the Alps date to this time too. Here we
362 see a clear increase in the estimated population in the model. In the transition to the Late Neolithic, we
363 know from the lakeshore settlements the so-called Horgen Gap (Hafner, 2005). This is also visible as a slight
364 decrease in the model. In another study (Heitz et al., 2021) we demonstrated that this is in fact probably not
365 a decline in population. Rather communities relocated their settlements to the hinterland of the large lakes
366 in times of stronger lake level rises due to climatic changes. In the Late Neolithic, associated with the Horgen
367 pottery, we then see a clear increase in the settlement intensity, which peaks and breaks off at the transition
368 to the Final Neolithic (Hafner, 2004). In the second half of the Early Bronze Age, during which lakeshores
369 were resettled to a smaller extend, there is again a clear increase in population size according to the model,
370 continuing until the Late Bronze Age. The general trends fit very well with the previous reconstructions of
371 population development for Switzerland (see eg. Lechterbeck et al., 2014), while offering higher precision and
372 higher resolution.

373 **7. Conclusions**

374 The key advance in the model we present is the ability to estimate, in absolute terms, past population
375 sizes and the uncertainty accompanying our present knowledge. These estimates can be a basis for further
376 studies where relative measures of population development are not helpful, such as long-term land use studies.

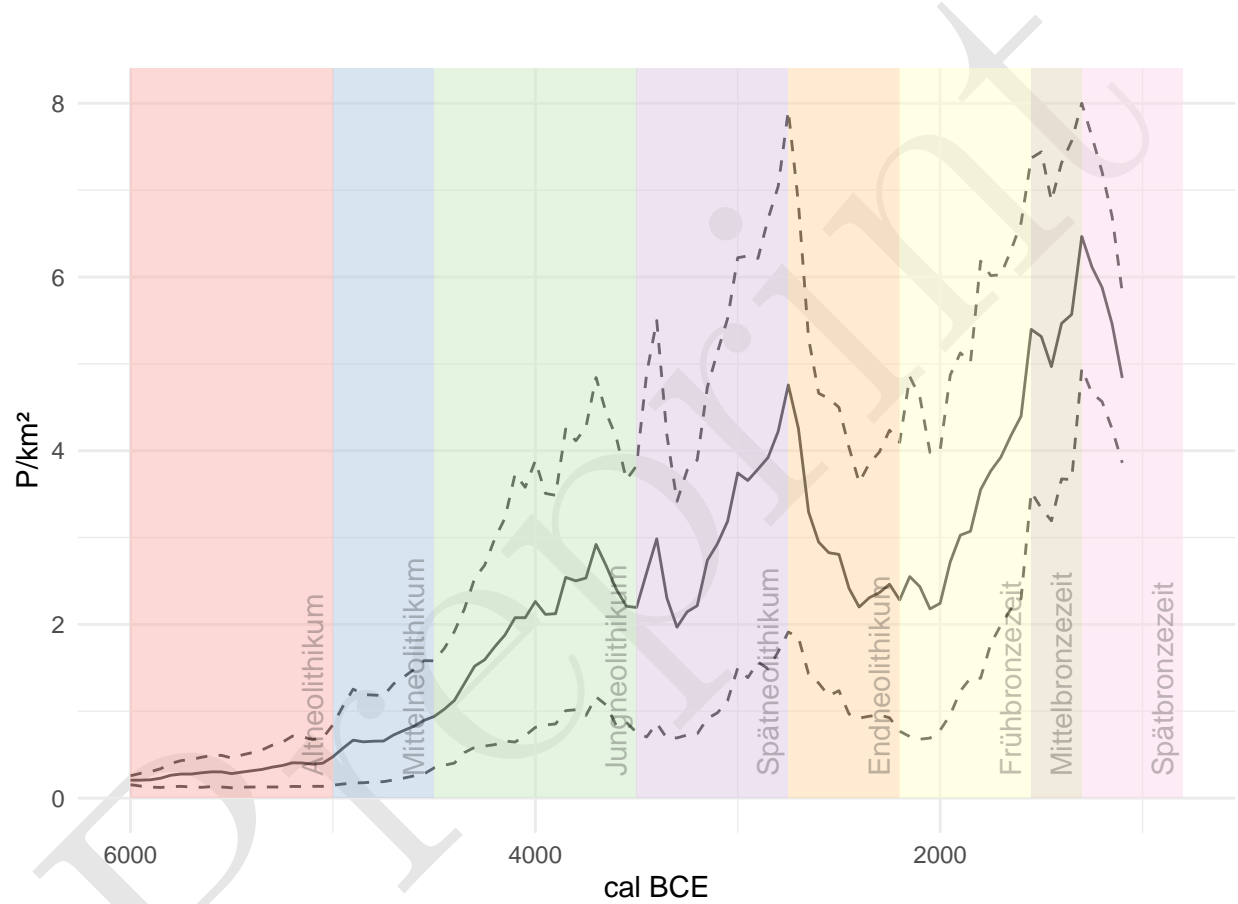


Figure 11: Estimate of population density in relation to the established chronology of the case study area north of the Swiss Alps.

377 Modelling of large-scale socio-ecological systems based on archaeological data does not have to rely deductive,
378 asynchronous population models (e.g. carrying capacity or ethnographic analogues).

379 We have also demonstrated that, with Bayesian hierarchical modelling, it is possible to achieve a true
380 multi-proxy analysis – as opposed to a juxtaposition of different indicators. This opens up the possibility
381 of quantitatively linking different records and assessing their credibility. We are also able to specifying a
382 confidence interval for the overall estimate. The result is a firmer basis for reconstructing population dynamics
383 and settlement patterns in prehistory.

384 Nevertheless, we consider this model as only the first step towards a more sophisticated Bayesian approach.
385 We have trusted the individual proxies in aggregate, without individualised measurement error. Our estimates
386 are based on a limited number of sources, almost all of which are subject to taphonomic biases in the
387 archaeological record. Consequently, we can only transform the model's prediction into an absolute estimate
388 of population density with predefined parameters: settlement size and the initial value of the reconstruction.
389 Overcoming this limitation would represent a major refinement of our approach.

390 Incorporating additional proxies independent of the immediate, time-dependent conditions of the archaeological
391 record could be one way to achieve this. These could be data on settlement sizes, parameters for economic-
392 ecological carrying capacity, demographic data from burial groups or archaeogenetic data on population sizes.
393 This data is available to varying degrees in different regions. On the Swiss Plateau, for example, we have little
394 data on human remains over large spans of prehistory, in contrast to the abundance of wetland settlements.

395 To apply this approach to other regions, the proxies we use here would have to be adapted to fit local
396 conditions and research histories. By means of large-scale modelling, however, it would be possible to
397 supplement gaps in the data in one region with data from another by regionalisation and a partial transfer of
398 information (partial pooling). Such an extension would be the next logical step in the improvement of the
399 model, to which end we hope to be able to contribute a further study in the near future.

400 8. Acknowledgements

401 Data collection were conducted as part of the project 'Beyond lake settlements' in the doctoral thesis of Julian
402 Laabs, funded by the SNF (project number 152862, PI Albert Hafner) and as part of the XRONOS project,
403 also funded by the SNSF (project number 198153, PI Martin Hinz). The development of the openness index
404 took place within the framework of the project Time and Temporality in Archaeology (project number 194326,
405 PI Caroline Heitz), inspired by the cooperation within the project QuantHum (project 169371, PI Marco
406 Conedera), both also funded by the SNSF. Jan Kolář was supported by a long-term research development
407 project (RV67985939) and by a grant from the Czech Science Foundation (19-20970Y). We also thank the
408 Institute of Archaeological Sciences of the University of Bern for its support and faith in the outcome of our
409 modelling project. Finally, we thank (already) the unknown reviewers for their helpful comments, which will
410 certainly improve this manuscript significantly.

411 9. References

- 412 Attenbrow, V., Hiscock, P., 2015. Dates and demography: Are radiometric dates a robust proxy for long-term
413 prehistoric demographic change? *Archaeology in Oceania* 50, 30–36. <https://doi.org/10.1002/arco.5052>
- 414 Bryant, J., Zhang, J.L., 2018. Bayesian Demographic Estimation and Forecasting. Chapman; Hall/CRC.
415 <https://doi.org/10.1201/9780429452987>
- 416 Carleton, W.C., Groucutt, H.S., 2021. Sum things are not what they seem: Problems with point-wise
417 interpretations and quantitative analyses of proxies based on aggregated radiocarbon dates. *The Holocene*
418 31, 630–643. <https://doi.org/10.1177/0959683620981700>
- 419 Childe, V.G. (Ed.), 1936. *Man Makes Himself*. Watts & Co., London.
- 420 Christian Lüthi, 2009. Mittelland (region).
- 421 Crema, E.R., 2022. Statistical Inference of Prehistoric Demography from Frequency Distributions of
422 Radiocarbon Dates: A Review and a Guide for the Perplexed. *Journal of Archaeological Method and*
423 *Theory*. <https://doi.org/10.1007/s10816-022-09559-5>
- 424 Crema, E.R., Bevan, A., 2021. Inference from large sets of radiocarbon dates: software and methods.
425 *Radiocarbon* 63, 23–39. <https://doi.org/10.1017/RDC.2020.95>
- 426 Crema, E.R., Shoda, S., 2021. A Bayesian approach for fitting and comparing demographic growth models
427 of radiocarbon dates: A case study on the Jomon-Yayoi transition in Kyushu (Japan). *PloS One* 16,
428 e0251695. <https://doi.org/10.1371/journal.pone.0251695>
- 429 David-Elbiali, M., 2000. La Suisse occidentale au IIe millénaire av. J.-C. : Chronologie, culture, intégration
430 européenne. *Cahiers d'archéologie romande*, Lausanne.
- 431 Ebersbach, R., Kühn, M., Stopp, B., Schibler, J., 2012. Die Nutzung neuer Lebensräume in der Schweiz
432 und angrenzenden Gebieten im 5. Jtsd. V. Chr. : Siedlungs- und wirtschaftsarchäologische Aspekte.
433 *Jahrbuch Archäologie Schweiz* 95, 7–34. <https://doi.org/10.5169/SEALS-392483>
- 434 French, J.C., Riris, P., Fernandéz-López de Pablo, J., Lozano, S., Silva, F., 2021. A manifesto for palaeodemography
435 in the twenty-first century. *Philosophical Transactions of the Royal Society B: Biological*
436 *Sciences* 376, 20190707. <https://doi.org/10.1098/rstb.2019.0707>
- 437 Hafner, A., 2005. Neolithikum: Raum/Zeit-Ordnung und neue Denkmodelle. *Archäologie im Kanton Bern*
438 6B, 431–498.
- 439 Hafner, A., 2004. Vom Spät- zum Endneolithikum. Wandel und Kontinuität um 2700 v. Chr. In *Mitteleuropa.*
440 - Vom Endneolithikum zur Frühbronzezeit: Wandel und Kontinuität zwischen 2400 und 1500 v.Chr, in:
441 Beier, H.J., Einicke, R. (Eds.), *Varia Neolithica. 3. Beiträge Zur Ur- Und Frühgeschichte Mitteleuropas.*
442 Beier&Beran, Weissbach, pp. 213–249.
- 443 Hafner, A., 1995. Die Frühe Bronzezeit in der Westschweiz. Funde und Befunde aus Siedlungen, Gräbern
444 und Horten der entwickelten Frühbronzezeit. *Staatlicher Lehrmittelverlag Bern* 1995, Bern.
- 445 Hassan, F.A., 1981. Demographic archaeology, Studies in archaeology. Academic Press, New York.
- 446 Heitz, C., Hinz, M., Laabs, J., Hafner, A., 2021. Mobility as resilience capacity in northern Alpine Neolithic
447 settlement communities. <https://doi.org/10.17863/CAM.79042>
- 448 Kintigh, K.W., Altschul, J.H., Beaudry, M.C., Drennan, R.D., Kinzig, A.P., Kohler, T.A., Limp, W.F.,
449 Maschner, H.D.G., Michener, W.K., Pauketat, T.R., Peregrine, P., Sabloff, J.A., Wilkinson, T.J., Wright,
450 H.T., Zeder, M.A., 2014. Grand challenges for archaeology. *Proceedings of the National Academy of*
451 *Sciences* 111, 879–880. <https://doi.org/10.1073/pnas.1324000111>
- 452 Kruschke, J.K., 2015. Doing Bayesian Data Analysis. Elsevier. <https://doi.org/10.1016/B978-0-12-405888-0.09999-2>
- 453 Laabs, J., 2019. Populations- und landnutzungsmodellierung der neolithischen und bronzezeitlichen
454 westschweiz (PhD thesis). Bern.
- 455 Lechterbeck, J., Edinborough, K., Kerig, T., Fyfe, R., Roberts, N., Shennan, S., 2014. Is Neolithic land
456 use correlated with demography? An evaluation of pollen-derived land cover and radiocarbon-inferred
457 demographic change from Central Europe. *The Holocene* 24, 1297–1307. <https://doi.org/10.1177/0959683614540952>
- 458 Martínez-Grau, H., Morell-Rovira, B., Antolín, F., 2021. Radiocarbon Dates Associated to Neolithic Contexts
459 (Ca. 5900 – 2000 Cal BC) from the Northwestern Mediterranean Arch to the High Rhine Area. *Journal*
460 *of Open Archaeology Data* 9, 1. <https://doi.org/10.5334/joad.72>
- 461 Morris, I., 2013. The measure of civilization: How social development decides the fate of nations. Princeton

- 464 University Press, Princeton.
- 465 Müller, J., Diachenko, A., 2019. Tracing long-term demographic changes: The issue of spatial scales. PLOS
466 ONE 14, e0208739. <https://doi.org/10.1371/journal.pone.0208739>
- 467 Nikulka, F., 2016. Archäologische Demographie. Methoden, Daten und Bevölkerung der europäischen Bronze-
468 und Eisenzeiten. Sidestone Press, Leiden.
- 469 Ramsey, C.B., 1995. Radiocarbon calibration and analysis of stratigraphy; the OxCal program. Radiocarbon
470 37, 425430.
- 471 Rick, J.W., 1987. Dates as Data: An Examination of the Peruvian Preceramic Radiocarbon Record. American
472 Antiquity 52, 55–73. <https://doi.org/10.2307/281060>
- 473 Riede, F., 2009. Climate and demography in early prehistory: Using calibrated (14)C dates as population
474 proxies. Human Biology 81, 309–337. <https://doi.org/10.3378/027.081.0311>
- 475 Schmidt, I., Hilpert, J., Kretschmer, I., Peters, R., Broich, M., Schiesberg, S., Vogels, O., Wendt, K.P.,
476 Zimmermann, A., Maier, A., 2021. Approaching prehistoric demography: Proxies, scales and scope of the
477 Cologne Protocol in European contexts. Philosophical Transactions of the Royal Society B: Biological
478 Sciences 376, 20190714. <https://doi.org/10.1098/rstb.2019.0714>
- 479 Shennan, S., 2000. Population, Culture History, and the Dynamics of Culture Change. Current Anthropology
480 41, 811–835.
- 481 Shennan, S., Downey, S.S., Timpson, A., Edinborough, K., Colledge, S., Kerig, T., Manning, K., Thomas,
482 M.G., 2013. Regional population collapse followed initial agriculture booms in mid-Holocene Europe.
483 Nature Communications 4, 2486. <https://doi.org/10.1038/ncomms3486>
- 484 Surovell, T.A., Byrd Finley, J., Smith, G.M., Brantingham, P.J., Kelly, R., 2009. Correcting temporal
485 frequency distributions for taphonomic bias. Journal of Archaeological Science 36, 1715–1724. <https://doi.org/10.1016/j.jas.2009.03.029>
- 486 Turchin, P., Brennan, R., Currie, T., Feeney, K., Francois, P., Hoyer, D., Manning, J., Marciniak, A., Mullins,
487 D., Palmisano, A., Peregrine, P., Turner, E.A.L., Whitehouse, H., 2015. Sesat: The Global History
488 Databank. Cliodynamics 6. <https://doi.org/10.21237/C7clio6127917>
- 489 Zimmermann, A., 2004. Landschaftsarchäologie II. Überlegungen zu prinzipien einer landschaftsarchäologie.

491 10. Author contributions

- 492 • *Martin Hinz*: Conceptualization, Methodology, Software, Validation, Formal analysis, Investigation,
493 Data Curation, Writing - Original Draft, Writing - Review & Editing, Visualization
494 • *Joe Roe*: Software, Validation, Writing - Review & Editing
495 • *Julian Laabs*: Investigation, Data Curation, Writing - Review & Editing
496 • *Caroline Heitz*: Conceptualization, Investigation, Writing - Review & Editing
497 • *Jan Kolář*: Conceptualization, Writing - Review & Editing

498 11. Colophon

499 This report was generated on 2022-05-30 10:16:37 using the following computational environment and
500 dependencies:

```
501 #> - Session info -----
502 #>   setting  value
503 #>   version R version 4.2.0 (2022-04-22)
504 #>   os        Manjaro Linux
505 #>   system   x86_64, linux-gnu
506 #>   ui        X11
507 #>   language (EN)
508 #>   collate   C
509 #>   ctype     de_DE.UTF-8
510 #>   tz        Europe/Zurich
511 #>   date      2022-05-30
512 #>   pandoc   2.17.1.1 @ /usr/bin/ (via rmarkdown)
513 #>
514 #> - Packages -----
515 #>   package * version date (UTC) lib source
516 #>   assertthat 0.2.1  2019-03-21 [1] CRAN (R 4.2.0)
517 #>   bitops     1.0-7  2021-04-24 [1] CRAN (R 4.2.0)
518 #>   bookdown   0.26   2022-04-15 [1] CRAN (R 4.2.0)
519 #>   brio       1.1.3   2021-11-30 [1] CRAN (R 4.2.0)
520 #>   cachem     1.0.6   2021-08-19 [1] CRAN (R 4.2.0)
521 #>   callr      3.7.0   2021-04-20 [1] CRAN (R 4.2.0)
522 #>   class      7.3-20  2022-01-16 [2] CRAN (R 4.2.0)
523 #>   classInt   0.4-3   2020-04-07 [1] CRAN (R 4.2.0)
524 #>   cli        3.3.0   2022-04-25 [1] CRAN (R 4.2.0)
525 #>   colorspace 2.0-3   2022-02-21 [1] CRAN (R 4.2.0)
526 #>   cowplot    * 1.1.1   2020-12-30 [1] CRAN (R 4.2.0)
527 #>   crayon     1.5.1   2022-03-26 [1] CRAN (R 4.2.0)
528 #>   curl       4.3.2   2021-06-23 [1] CRAN (R 4.2.0)
529 #>   DBI        1.1.2   2021-12-20 [1] CRAN (R 4.2.0)
530 #>   desc       1.4.1   2022-03-06 [1] CRAN (R 4.2.0)
531 #>   devtools   2.4.3   2021-11-30 [1] CRAN (R 4.2.0)
532 #>   digest     0.6.29  2021-12-01 [1] CRAN (R 4.2.0)
533 #>   dplyr      1.0.9   2022-04-28 [1] CRAN (R 4.2.0)
534 #>   e1071     1.7-9   2021-09-16 [1] CRAN (R 4.2.0)
535 #>   ellipsis   0.3.2   2021-04-29 [1] CRAN (R 4.2.0)
536 #>   evaluate   0.15    2022-02-18 [1] CRAN (R 4.2.0)
537 #>   fansi      1.0.3   2022-03-24 [1] CRAN (R 4.2.0)
538 #>   farver     2.1.0   2021-02-28 [1] CRAN (R 4.2.0)
539 #>   fastmap   1.1.0   2021-01-25 [1] CRAN (R 4.2.0)
540 #>   foreign   0.8-82  2022-01-16 [2] CRAN (R 4.2.0)
```

```

541 #> fs           1.5.2   2021-12-08 [1] CRAN (R 4.2.0)
542 #> generics     0.1.2   2022-01-31 [1] CRAN (R 4.2.0)
543 #> ggmap        * 3.0.0   2019-02-05 [1] CRAN (R 4.2.0)
544 #> ggplot2      * 3.3.6   2022-05-03 [1] CRAN (R 4.2.0)
545 #> ggrepel       * 0.9.1   2021-01-15 [1] CRAN (R 4.2.0)
546 #> ggsn         * 0.5.0   2019-02-18 [1] CRAN (R 4.2.0)
547 #> glue          1.6.2   2022-02-24 [1] CRAN (R 4.2.0)
548 #> gtable        0.3.0   2019-03-25 [1] CRAN (R 4.2.0)
549 #> here          * 1.0.1   2020-12-13 [1] CRAN (R 4.2.0)
550 #> highr         0.9     2021-04-16 [1] CRAN (R 4.2.0)
551 #> htmltools     0.5.2   2021-08-25 [1] CRAN (R 4.2.0)
552 #> httr          1.4.3   2022-05-04 [1] CRAN (R 4.2.0)
553 #> jpeg          0.1-9   2021-07-24 [1] CRAN (R 4.2.0)
554 #> KernSmooth    2.23-20  2021-05-03 [2] CRAN (R 4.2.0)
555 #> knitr         1.39    2022-04-26 [1] CRAN (R 4.2.0)
556 #> labeling       0.4.2   2020-10-20 [1] CRAN (R 4.2.0)
557 #> lattice        0.20-45  2021-09-22 [2] CRAN (R 4.2.0)
558 #> lifecycle      1.0.1   2021-09-24 [1] CRAN (R 4.2.0)
559 #> magrittr       2.0.3   2022-03-30 [1] CRAN (R 4.2.0)
560 #> maptools       1.1-4   2022-04-17 [1] CRAN (R 4.2.0)
561 #> memoise        2.0.1   2021-11-26 [1] CRAN (R 4.2.0)
562 #> munsell        0.5.0   2018-06-12 [1] CRAN (R 4.2.0)
563 #> pillar         1.7.0   2022-02-01 [1] CRAN (R 4.2.0)
564 #> pkgbuild       1.3.1   2021-12-20 [1] CRAN (R 4.2.0)
565 #> pkgconfig      2.0.3   2019-09-22 [1] CRAN (R 4.2.0)
566 #> pkgload         1.2.4   2021-11-30 [1] CRAN (R 4.2.0)
567 #> plyr           1.8.7   2022-03-24 [1] CRAN (R 4.2.0)
568 #> png             0.1-7   2013-12-03 [1] CRAN (R 4.2.0)
569 #> prettyunits    1.1.1   2020-01-24 [1] CRAN (R 4.2.0)
570 #> processx       3.5.3   2022-03-25 [1] CRAN (R 4.2.0)
571 #> proxy          0.4-26  2021-06-07 [1] CRAN (R 4.2.0)
572 #> ps              1.7.0   2022-04-23 [1] CRAN (R 4.2.0)
573 #> purrr          0.3.4   2020-04-17 [1] CRAN (R 4.2.0)
574 #> R6              2.5.1   2021-08-19 [1] CRAN (R 4.2.0)
575 #> RColorBrewer   1.1-3   2022-04-03 [1] CRAN (R 4.2.0)
576 #> Rcpp            1.0.8.3  2022-03-17 [1] CRAN (R 4.2.0)
577 #> remotes         2.4.2   2021-11-30 [1] CRAN (R 4.2.0)
578 #> rgdal           1.5-32  2022-05-09 [1] CRAN (R 4.2.0)
579 #> RgoogleMaps    1.4.5.3  2020-02-12 [1] CRAN (R 4.2.0)
580 #> rjson           0.2.21  2022-01-09 [1] CRAN (R 4.2.0)
581 #> rlang           1.0.2   2022-03-04 [1] CRAN (R 4.2.0)
582 #> rmarkdown        2.14    2022-04-25 [1] CRAN (R 4.2.0)
583 #> rnaturalearth  * 0.1.0   2017-03-21 [1] CRAN (R 4.2.0)
584 #> rprojroot       2.0.3   2022-04-02 [1] CRAN (R 4.2.0)
585 #> rstudioapi      0.13    2020-11-12 [1] CRAN (R 4.2.0)
586 #> s2              1.0.7   2021-09-28 [1] CRAN (R 4.2.0)
587 #> scales          1.2.0   2022-04-13 [1] CRAN (R 4.2.0)
588 #> sessioninfo    1.2.2   2021-12-06 [1] CRAN (R 4.2.0)
589 #> sf               * 1.0-7   2022-03-07 [1] CRAN (R 4.2.0)
590 #> sp               * 1.4-7   2022-04-20 [1] CRAN (R 4.2.0)
591 #> stringi          1.7.6   2021-11-29 [1] CRAN (R 4.2.0)
592 #> stringr          1.4.0   2019-02-10 [1] CRAN (R 4.2.0)
593 #> testthat         3.1.4   2022-04-26 [1] CRAN (R 4.2.0)
594 #> tibble          3.1.7   2022-05-03 [1] CRAN (R 4.2.0)

```

```
595 #> tidyverse      1.2.0  2022-02-01 [1] CRAN (R 4.2.0)
596 #> tidyselect     1.1.2  2022-02-21 [1] CRAN (R 4.2.0)
597 #> units          0.8-0  2022-02-05 [1] CRAN (R 4.2.0)
598 #> usethis        2.1.5  2021-12-09 [1] CRAN (R 4.2.0)
599 #> utf8           1.2.2  2021-07-24 [1] CRAN (R 4.2.0)
600 #> vctrs          0.4.1  2022-04-13 [1] CRAN (R 4.2.0)
601 #> withr          2.5.0  2022-03-03 [1] CRAN (R 4.2.0)
602 #> wk              0.6.0  2022-01-03 [1] CRAN (R 4.2.0)
603 #> xfun            0.31   2022-05-10 [1] CRAN (R 4.2.0)
604 #> yaml            2.3.5  2022-02-21 [1] CRAN (R 4.2.0)
605 #>
606 #> [1] /home/martin/R/x86_64-pc-linux-gnu-library/4.2
607 #> [2] /usr/lib/R/library
608 #>
609 #> -----
```